ChemPubSoc Europe

DOI: 10.1002/ejic.201900742

EurJIC European Journal of Inorganic Chemistry

Full Paper

Nanoimprint of Phospholes

Tailoring Phospholes for Imprint of Fluorescent 3D Structures

Fabian Roesler,[a] Burhan Kaban,[b] Dieter Klintuch,[a] Uh-Myong Ha,[b] Clemens Bruhn,[a] Hartmut Hillmer,*[b] and Rudolf Pietschnig*[a]

Dedicated to Professor Dr. Reinhold Tacke on the occasion of his 70th birthday

Abstract: PMMA based polymer blends have been infused with luminescent phospholes and have been structured via nanoimprint. While symmetrically substituted phospholes are prone to crystallization and phase separation, structural modification of the phosphole backbone in the α- and β-positions has been explored, which prevents these issues; a structural explanation for this is suggested. Best phase integrity has been obtained for β-silyl-substituted phospholes, which were implemented in thin films and beads. The emission wavelengths of the phospholes are shifted bathochromically in the polymer matrix as compared to the neat compounds featuring emission bands near 500 nm. This enables tracking of the fluorescent beads using standard fluorescence microscopy.

Introduction

Phospholes are fundamental and relatively simple functional molecules with fascinating properties useful in designing molecular electronic devices.[1] Promising recent developments target applications spanning from OLEDs over photovoltaic devices to bio-imaging to name just a few.[2] Phospholes and their derivatives offer a multitude of opportunities for structural variation which allows tuning of the electronic structure pertinent to their photophysical features such as fluorescence.[3] The lipophilic nature of phospholes should be well suited to allow their immersion into non-polar polymer blends for nanoimprint lithography (NIL). NIL is a powerful time and cost-efficient method for the preparation of reproducible and uniform surface patterns or polymer beads. Since its early demonstration in 1996, NIL has been continuously developed and its use has been implemented within a wide variety of fields and applications.[4] As a proof of concept fluorescent NIL beads have been prepared using fluorescein as a simple molecular fluorophore.[4d,5] Fluorescent metal ions such as lanthanides are difficult to incorporate into polymer blends owing to their polar properties. Nevertheless, NIL patterned fluorescent beads containing europium(III)oxide nanoparticles have been developed recently where phase separation could be avoided at low particle loadings.[6] Given the proven flexibility of the phosphole scaffold in tuning the luminescence properties of molecules we set out to explore the possibility to infuse the nanoimprinted polymer with phospholes as fluorescent molecules (Scheme 1). Here we report our results in preparing the first imprinted 3D structures and beads containing phospholes along with variation of the molecular structure to avoid phase separation between fluorophore and polymer blend during the NIL process.

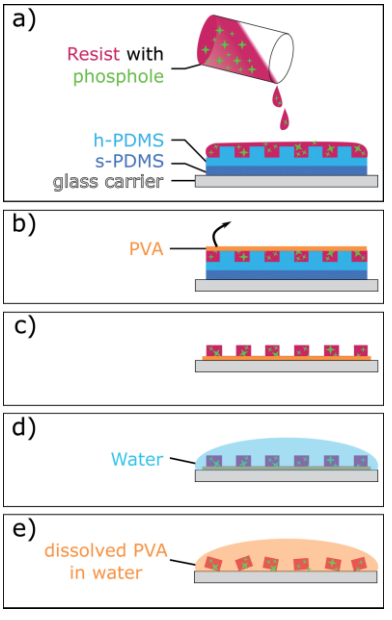

Scheme 1. Fabrication of 3D structures via reverse nanoimprint lithography.

[a] Institute of Chemistry and Center for Interdisciplinary Nanostructure Science and Technology (CINSaT), University of Kassel, Heinrich-Plett-Straße 40, 34132 Kassel, Germany
E-mail: pietschnig@uni-kassel.de
http://www.uni-kassel.de/go/hym

[b] Institute of Nanostructure Technologies and Analytics (INA) and Center for Interdisciplinary Nanostructure Science and Technology (CINSaT), University of Kassel, Heinrich-Plett-Straße 40, 34132 Kassel, Germany
http://www.te.ina-kassel.de

Supporting information and ORCID(s) from the author(s) for this article are available on the WWW under https://doi.org/10.1002/ejic.201900742.

Results and Discussion

NIL processes require optimized polymer blends to ensure complete filling of the mold especially when producing complex shapes. The literature known triphenylphosphole **1** was used as a first example owing to its high fluorescence quantum yield at an emission wavelength of 459 nm and its chemical robustness.[7] However, during the spin coating process phase separation was observed for typical imprint mixtures of 4 % PMMA in ethyl lactate with phosphole **1** at a concentration of 20 g/L leading to crystalline **1**. We concluded that the relatively high molecular symmetry of **1** may be responsible for its tendency to crystallize. Using a recently reported general synthetic methodology to phospholes which are mono- or bi-functional in the β-position,[8] we prepared a modified triphenylphosphole derivative **2** with an additional trimethylsilyl unit in the β-position of the central ring to lower the molecular symmetry (Scheme 2).

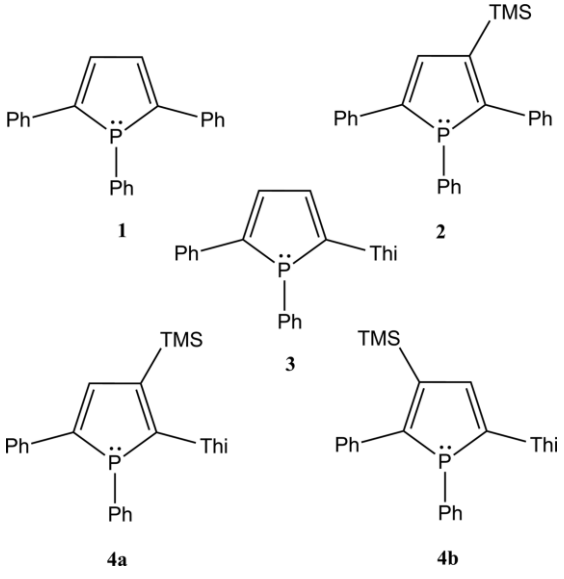

Scheme 2. Molecular structures of phospholes used in this study (Ph = phenyl, Thi = thienyl, TMS = trimethylsilyl).

Repeating the above-mentioned spin coating experiment with polymer mixtures containing **2** instead of **1** resulted in uniform films with a layer thickness of 106 nm at a spincoating speed of 4000 rpm, which compares to a layer thickness of 80 nm for pure PMMA at the same conditions.[9] Besides unsymmetric substitution in β-position, we set out to vary the substitution pattern in the α-position such as in phosphole **3** which likewise has a reduced molecular symmetry. Phosphole **3** has not been described in the literature so far and was prepared using the above-mentioned methodology previously developed by us (Scheme 3). Spin coating of **3** immersed in PMMA ethyl lactate solution again resulted in phase separation and crystallization of the respective phosphole.

Since the unsymmetric substitution pattern was more efficient in the β-position **(2)** than in the α-position **(3)** in terms of phase mixing behavior with PMMA, we investigated the role of unsymmetrical substitution pattern in both α- and β-position of the phospholes. To this end, we prepared modified phosphole derivative **4** with an unsymmetric substitution pattern in α-position and a trimethylsilyl unit in the β-position of the central ring according to Scheme 3. Direct addition of Ph-PTMSLi to the diyne results in better yields than reacting the β-lithiated phosphole intermediate depicted in Scheme 3 with trimethylsilyl chloride, which likewise results in formation of **4**.

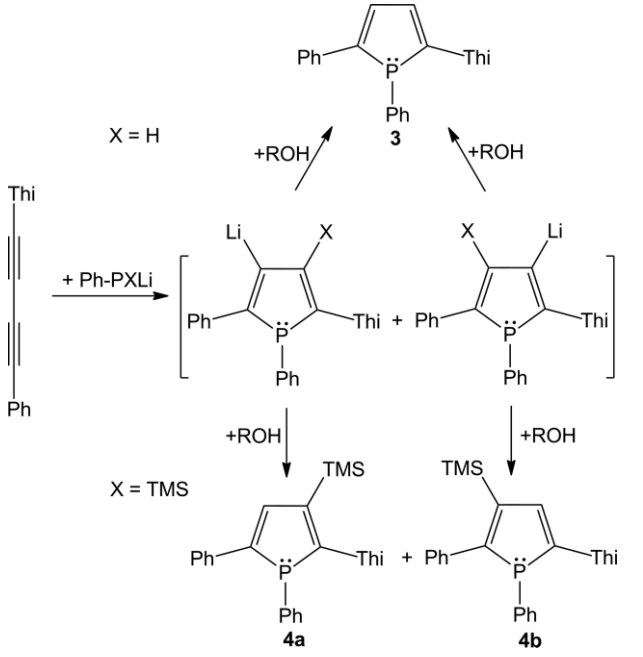

Scheme 3. Synthesis of phospholes **3**, **4a** and **4b** (Ph = phenyl, Thi = thienyl, TMS = trimethylsilyl, X = H or TMS, R = ethyl, methyl, H).

Phosphole **4** is obtained as mixture of isomers **4a** and **4b** depending of the position of the trimethylsilyl unit either on the phenyl or thienyl-substituted side of the phosphole ring. Isomers **4a** and **4b** show practically identical ^{31}P NMR resonances at 24.5 ppm while the ^{29}Si resonances are well separated (($\delta(^{29}Si)$ = –7.5 and –7.6 ppm). We did not succeed in in separating isomers **4a** and **4b** by chromatography. Nevertheless, the ratio of isomers (roughly 4:1) is so distinct to allow assignment of sets of NMR signals to the respective isomers. One may speculate that the major isomer is likely to be the sterically less hindered isomer **4a** in which the TMS group is neighboring the five membered thienyl ring for which also a single crystal suitable for X-ray diffraction has been obtained (Figure 1). Since the photophysical properties were indistinguishable for **4a** and **4b** (vide infra), we used the mixture of both for imprint purposes which is referred to as **4**. Spin coating of phosphole **4** featuring unsymmetric substitution in α- and β-position was successful in combination with polymer PMMA without problems of phase separation or crystallization. Both β-silylated phospholes **2** and **4** are phase-stable in the imprint polymer blend and therefore suitable candidates for nano-imprint experiments. In contrast, the proclivity of phospholes **1** and **3** to undergo phase separation and crystallization makes them unsuitable for imprint processes based on PMMA polymer blends.

Potential reasons for the different phase mixing behavior may be derived from the molecular geometry in silylated **2** and **4** vs. their non silylated analogues **1** and **3**. While unsilylated phospholes **1** and **3** feature a near coplanar arrangement of the

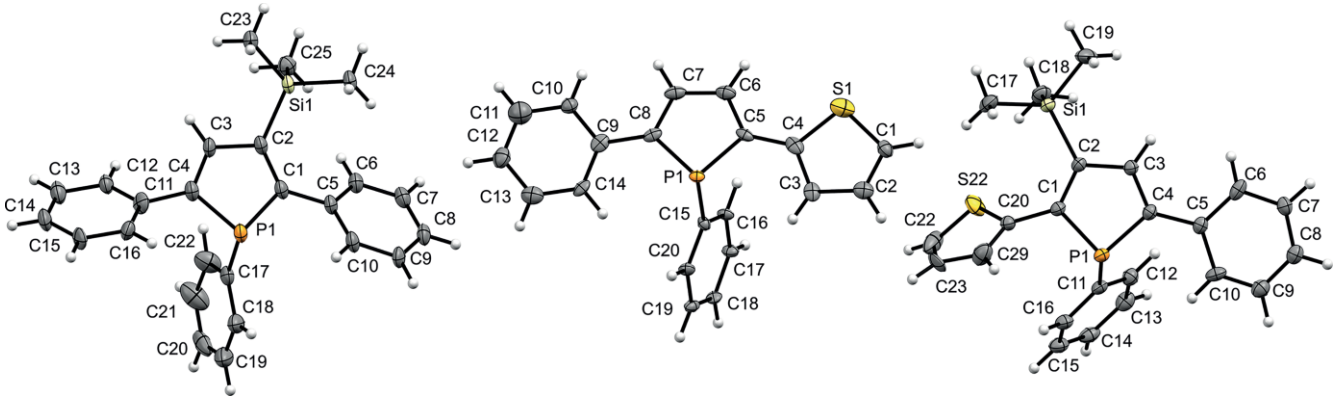

Figure 1. Molecular structures of **2** (left), **3** (middle) and **4a** (right) in the solid state. Thermal ellipsoids drawn at 30 % probability level.

central phosphole ring with the adjacent aromatic rings in α-position (**1**: 4.6(1)° and 8.0(1)°,[10] **3**: 6.9(3)° and 3.5(3)°), the presence of the TMS group in direct vicinity would be expected to entail a larger dihedral angle between the neighboring aromatic ring and the phosphole ring in **2** and **4a** owing to steric repulsion. This is corroborated by X-ray diffraction in the solid state (Figure 1), the presence of a β-TMS induces significant twisting of cyclic α-substituents in **4a** and **2**. Owing to disorder the structural parameters have to be interpreted with caution, nevertheless the thienyl ring in **4a** is twisted significantly more (49.7(3)°) than its phenyl congener on the opposite side (8.4(2)°). Similarly, in **2** the twisting of the phenyl group neighboring the TMS group is significantly larger (30.6(2)°) than in the β-unsubstituted case, while the one on the opposite side is disordered over two sites.

The structural modification of the phosphole backbone does not only affect the phase mixing behavior, but also the photophysical properties of these compounds. While the symmetrically substituted phosphole **1** shows an emission at 459 nm as a neat solid, this band shows a slight bathochromic shift to 474 nm upon silyl substitution in **2**. In the same vein, unsilylated phosphole **3** with unsymmetric substitution in α-position shows a further bathochromic emission wavelength of 487 nm with a quantum yield of 34 % in solution (absolute method based on integrating sphere). The combination of a thienyl group in α-position and a trimethylsilyl unit in the β-position of **4** entails the most distinct bathochromic shift with an emission wavelength of 490 nm along with a quantum yield of 6 % in solution (absolute method based on integrating sphere). Prior to the imprint of structures and beads, the luminescence properties of the thin films of the polymer blends containing **2** and **4** have been studied in the UV/Vis region based on excitation and emission spectra. The polymer film containing **2** shows a maximum absorption at 359 nm and an emission maximum at 506 nm which represents a bathochromic shift of ca. 32 nm as compared to the same phosphole as a neat substance (Figure 2).

For blends containing phosphole **4**, the maximum absorption is at 388 nm, while the emission shows a maximum at 542 nm which is red-shifted by 55 nm as compared to the neat phosphole (Figure 3). The quantum yields for the imprinted phospholes are 38 % (**2**) and 5 % (**4**) (absolute method based on integrating sphere). These values demonstrate that no oxidation of the phospholes took place during the spin coating procedure. The same holds true even for prolonged exposure of the resulting phosphole containing thin films to air, while the neat phospholes **2** and **4** are oxidized within one week under identical conditions.

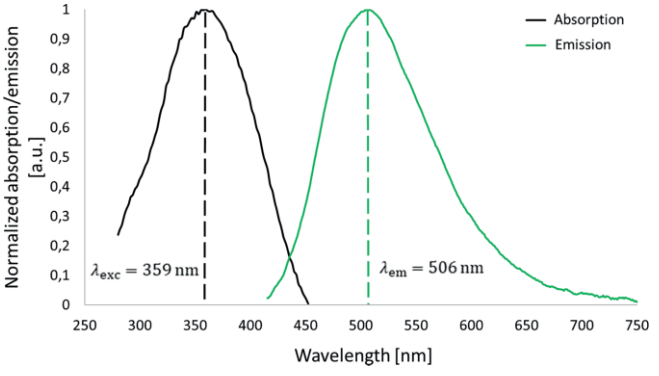

Figure 2. Excitation and emission spectra in the UV/Vis region of a thin film containing phosphole **2**. The excitation wavelength (359 nm, dotted line) was set to the maximum of the absorption (black line), whereas the maximum emission (green line) is at 506 nm.

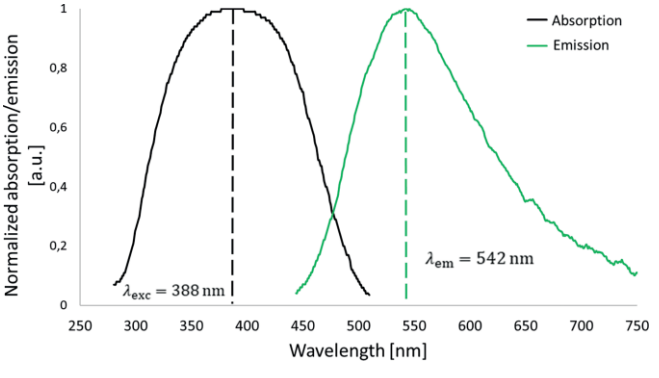

Figure 3. Excitation and emission spectra in the UV/Vis region of a thin film containing phosphole **4**. The excitation wavelength (388 nm, dotted line) was set to the maximum of the absorption (black line), whereas the maximum emission (green line) is at 542 nm.

Nanoimprinted structures and beads were fabricated from polymer blends containing phospholes **2** and **4** by the reversal

NIL technique.[6] For the fabrication of a master template we used a combination of electron beam lithography and reactive ion etching to produce rectangular 3D structures.[6] The rectangular bars own dimensions of 2 μm × 5 μm × 1 μm (width x length x height) as determined following a previously described procedure.[6] Prior to the NIL process phospholes **1–4** were immersed in a PMMA based photoresist. From these mixtures, polymer films were prepared using spin coating to explore the flow behavior based on their rheological properties. Our investigations revealed that for the phosphole polymer blends a delay time of 5 min and a spin-coating speed of 500 rpm for **2** and **4** are optimized fabrication parameters. Following our established methodology, imprinted beads are obtained attached to a thin residual layer. It was further possible to implement an extraction foil consisting of water soluble PVA between beads and residual layer which is soluble in suitable solvents, e.g. water, in order to release the imprinted beads.

Owing to the luminescent nature of the phosphole containing imprinted structures and beads investigation of the latter with fluorescence microscopy (FM) is feasible. FM illustrates the arrangement of the fluorescent beads before and after detachment of the fluorescent beads from the supporting layer (Figure 4). The imprinted beads show intense fluorescence especially at the short edges of the columnar structures. Reasons for this may be a consequence of one or a combination of several of the following aspects: (i) refractive index contrast related internal total reflection at the longer side related to waveoptic phenomena at the shorter side (waveguiding), (ii) different diffraction at the different apertures, (iii) interface orientation dependent orientation of the particles within the fluorescence microscope, (iv) a size dependent resonance phenomenon or (v) a consequence of inhomogeneous polymer filling or shape deviations (rims). A closer investigation of the relative contributions of the above mentioned mechanisms exceeds, however, the scope of the underlying study. Remarkably, the polymer matrix protects the phosphole sufficiently from oxidation, and the fluorescent properties are retained at ambient conditions in air over prolonged time.

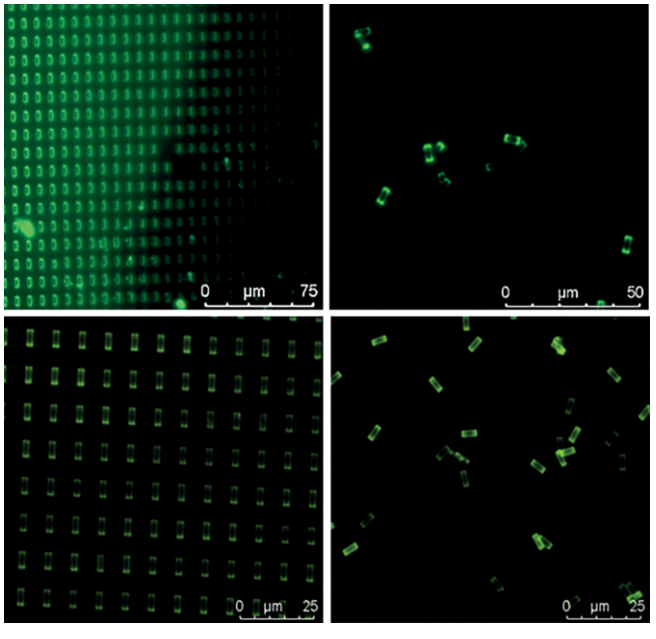

Figure 4. FM images of the imprinted phospholes **2** (top) and **4** (bottom) with an incorporation concentration of 4 g/L. Left: imprinted structures on PVA-layer. Right: free imprinted structures after dissolving PVA in water. The luminescent structures were excited at 360–380 nm.

Conclusions

Our results show that silyl substitution in the β-position of phospholes is more efficient than variation of the substitution pattern in in the α-position in preventing phase separation and crystallization of the phosphole from PMMA polymer blends for 3D imprint processes. The polymer matrix protects the phospholes from oxidation during the imprint process, as well as in the final beads. This approach opens the way to implement the large body of phosphole based luminescent materials into 3D imprinted structures, patterns and beads. Moreover, we intend to take advantage of the chiral nature of the β-silylphospholes to explore the interaction of such imprinted structures with circularly polarized light in future investigations.

Experimental Section

Compounds **1** and **2** have been prepared according to published procedures.[8,11] For the synthesis of phospholes **3** and **4** the procedure was slightly changed. Solvents were dried and freshly distilled from Na/K-alloy when necessary. Phenylphosphane was synthesized by reduction of dichlorophenylphosphane with LAH.[12] 1-Thienyl-4 phenyl-butadiyne was prepared according to a published procedure.[14] All other reagents have been purchased from Sigma Aldrich, ABCR or TCI and were used without further purification.

Synthetic Procedures

Synthesis of Phosphole 3: A solution of phenylphosphane (0.42 g, 3.85 mmol, 1 equiv.) in anhydrous THF (80 mL) was placed in a 250 mL Schlenk flask and cooled to –60 °C. *n*BuLi (1.5 mL, 3.85 mmol, 1 equiv.) was added to the stirring mixture. After 1.5 h 1-phenyl-4-thienylbuta-1,3-diyne (0.80 g, 3.85 mmol, 1 equiv.) was dissolved in anhydrous THF (40 mL) and added dropwise to the stirring solution. The resulting black solution was stirred at room temperature for 30 min. Finally, ethanol was added to quench the reaction. The solvent was evaporated under vacuum and the residue loaded on a column of silica gel with Pentane and DCM (20:1) as eluent. After drying, the purified phosphole 3 was obtained as a yellow solid; yield 0.72 g (59 %). ^{1}H-NMR (400 MHz, CD_2Cl_2): δ = 7.57–7.50 (m, 2 H), 7.47–7.42 (m, 2 H), 7.33–7.13 (m, 8 H), 7.06–6.89 (m, 2H). $^{13}C\{^{1}H\}$-NMR (100.56 MHz, CD_2Cl_2): δ = 150.5 (d, J = 1.9 Hz), 144.8 (d, J = 2.2 Hz), 140.3 (d, J = 2.3 Hz), 136.0 (d, J = 16.8 Hz), 133.9 (d, J = 20.4 Hz), 132.3 (d, J = 8.3 Hz), 131.6 (d, J = 8.4 Hz), 130.9 (d, J = 9.2 Hz), 130.0 (d, J = 1.6 Hz), 128.9 (d, J = 8.8 Hz), 128.7 (d, J = 1.1 Hz), 127.8 (2), 127.3 (s), 126.1 (d, J = 9.8 Hz), 124.5 (d, J = 1.5 Hz), 124.2 (d, J = 7.5 Hz). $^{31}P\{^{1}H\}$-NMR (202.30 MHz, CD_2Cl_2): δ = 4.7 (s). Elemental analysis (%): calculated: C 75.45, H 4.75, found: C 75.53, H 4.761. MS (APCI-HR) *m/z*: 319.070301 $[M + H]^+$, calculated: 319.07048.

Synthesis of Phosphole 4: A solution of phenylphosphane (0.30 g, 2.75 mmol, 1 equiv.) in anhydrous DME (20 mL) was placed in a 100 mL Schlenk tube and cooled to –60 °C. *n*BuLi (1.1 mL, 2.75 mmol, 1 equiv.) was added to the stirring mixture. After 40 min

the reaction mixture was quenched with TMSCl (0.3 mL, 2.75 mmol, 1 equiv.) and lithiated with *n*BuLi (1.1 mL, 2.75 mmol, 1 equiv.) again. The mixture was stirred for 70 min. 1-Phenyl-4-thienylbuta-1,3-diyne (0.57 g, 2.75 mmol, 1 equiv.) was dissolved in anhydrous DME (25 mL) and added dropwise to the stirring solution. The resulting black solution was stirred at room temperature for 30 min. Finally, ethanol was added to quench the reaction. The solvent was evaporated under vacuum and the residue loaded on a column of silica gel with Pentane and DCM (20:1) as eluent. After drying, the purified phosphole 4 was obtained as a transparent green-yellow wax; yield 0.62 g (60 %). ^{1}H-NMR (400 MHz, CD_2Cl_2): δ = 7.74–7.69 (m, 2 H), 7.62 (d, $^{3}J_{H,P}$ = 10.7 Hz, 1 H), 7.50–7.24 (m, 10 H), 7.18–7.01 (m, 2H) 0.42 (s, 7.5 H, Si(CH_3)$_3$), 0.30 (s, 1.5 H, Si(CH_3)$_3$). ^{31}P{^{1}H}-NMR (202.30 MHz, CD_2Cl_2): δ = 24.5 (s). ^{29}Si{^{1}H}-NMR (99.28 MHz, CD_2Cl_2): δ = –7.52 (d, $^{3}J_{Si\text{-}p}$ = 3.8 Hz), –7.64 (d, $^{3}J_{Si\text{-}p}$ = 3.3 Hz). Elemental analysis (%): calculated: C 70.73, H 5.94, found: C 70.45, H 6.10. MS (APCI-HR) *m/z*: 391.11028. [M + H]$^{+}$, calculated: 391.11001.

Isomer 1: ^{13}C{^{1}H}-NMR (100.56 MHz, CD_2Cl_2): δ = 163.0 (d, *J* = 6.4 Hz), 150.0 (d, *J* = 5.3 Hz), 149.6 (d, *J* = 5.8 Hz), 144.6 (s), 141.0 (d, *J* = 21.3 Hz), 138.0 (d, *J* = 12.7 Hz), 134.9 (d, *J* = 19.4 Hz), 134.4 (d, *J* = 20.0 Hz), 131.4 (d, *J* = 10.8 Hz), 129.7 (d, *J* = 7.5 Hz), 129.3 (s), 128.5 (s), 127.8 (s), 127.0 (d, *J* = 6.8 Hz), 125.1 (d, *J* = 6.9 Hz), 125.0 (d, *J* = 1.5 Hz), 0.8 (d, *J* = 1.5 Hz).

Isomer 2: ^{13}C{^{1}H}-NMR (100.56 MHz, CD_2Cl_2): δ = 155.2 (d, *J* = 3.5 Hz), 151.1 (d, *J* = 2.3 Hz), 148.7 (d, *J* = 4.6 Hz), 144.3 (d, *J* = 0.7 Hz), 141.3 (d, *J* = 23.7 Hz), 138.8 (d, *J* = 11.9 Hz), 137.2 (d, *J* = 16.7 Hz), 134.4 (d, *J* = 18.9 Hz), 131.6 (d, *J* = 10.0 Hz), 130.3 (d, *J* = 1.8 Hz), 129.4 (s), 128.0 (s), 127.1 (d, *J* = 9.2 Hz), 126.4 (d, *J* = 2.0 Hz), 124.9 (d, *J* = 6.6 Hz), 124.8 (d, *J* = 6.9 Hz), 0.7 (d, *J* = 1.1 Hz).

Imprint Procedure

Fabrication of Nanoimprinted Beads: For the fabrication of fluorescent nanoimprinted beads, a reversal NIL (rNIL) process with PMMA 639.04 K (supplied by Allresist GmbH, Germany) was used. At first, 30 µL of polymer blend is applied to the stamp using a microliter pipette. After the application a filling time is introduced giving the polymer blend time to fill up the stamp structures. During our investigations the filling time and the concentration range of phosphole were varied from 1 min. to 10 min. and 4 g/L to 20 g/L. In contrast to the normal NIL process the stamp is coated with a polymer and the excess material was removed with a spin-coating speed of 500 rpm. This results in a thin residual layer, which does not need to be removed. For separation of the polymer beads from the stamp an extraction foil was formed by applying a PVA solution on the stamp and hardening at 85 °C for 30 min. The extraction foil has been dissolved in water, thus releasing the imprinted beads.

Fabrication of master template and stamp

The master template was fabricated using electron beam lithography from (Raith eLine Plus). By using a positive resist (PMMA 692.03 K Allresist GmbH, Germany) rectangular holes were patterned exposing the silicon substrate (with an electron dose of 120 µC/cm^2). After the development of the patterns in a methyl isobutyl ketone and isopropyl alcohol solution (1:3) for 3 min. a (50 nm) chromium hard mask was evaporated to the substrate using electron beam vapour deposition. To transfer the patterns into the substrate a RIE step using Oxford Plasmalab 100 was used. The etching process included C_4F_8 (28 sccm) and O_2 (10 sccm) and results in an etching rate of 0.8 nm/s. The dimensions of the master template were verified using SEM and white light interferometry and resulted in the dimensions of (width: 2.377 ± 0.06 µm x length: 5.290 ± 0.03 µm and height: 1.024 ± 0.001 µm).

For the stamp fabrication an anti-sticking layer was applied to the silicon master template at 120 °C for 1 h. This layer consists of perfluorodecyltrichlorosilane (FDTS) (Ab111155, ABCR GmbH). Subsequently, a polydimethylsiloxane PDMS stamp is molded from the master template, which consists of three materials: i) hard-PDMS, ii) soft-PDMS and iii) glass carrier, which is used for handling purposes.[6,15]

i) was prepared by mixing two components (A and B). Component A consists of 100 g trimethylsiloxy terminated vinylmethylsiloxane-dimethylsiloxane copolymer (AB112958, ABCR GmbH), 0.38 g platinum-1,3-divinyltetramethyldisiloxane (Karstedt's catalyst, AB153234, ABCR GmbH) and 1.27 g 2,4,6,8-tetramethyltetravinylcyclotetrasiloxane (AB171991, ABCR GmbH). The second component B consists of methylhydrosiloxane-dimethylsiloxane copolymer (AB109380, ABCR GmbH).

ii) was prepared by mixing the base and the curing agent of Sylgard 184 in a ratio of 10:1 (Dow Corning). By spincoating the master template with 1000 rpm for 20 s a thin layer of hard-PDMS was applied and baked afterwards for 20 min at 65 °C. The soft-PDMS is then applied to the coated master template and covered with a glass carrier, which is set to a height of (1.00±0,01) mm with spacers and cured on a hotplate at 65 °C for 3 days before separating it mechanically from the silicon master template. This composition of the stamp enables a high precision accuracy of the shape down to sub 100-nanometer feature size as well as high durability.[15]

Characterization

Nuclear Magnetic Resonance (NMR): NMR measurements were done on Varian 400 MHz and 500 MHz spectrometers.

Luminescence Spectra: Excitation and emission spectra as well as luminescent quantum yields (absolute method) measurements were carried out using a Hamamatsu C11347 system. The solid-state samples were applied on a quartz plate (10 × 10 mm) and measured in an integrating sphere. An empty quartz plate of the same size was used for reference. For the refinement of the data ORIGIN 2017 was used.

Elemental Analysis (EA): Elemental analyses were performed with a HEKAtech Euro EA CHNS elemental analyzer.

Mass spectrometry (MS). APCI-mass spectra (Atmospheric pressure chemical ionization) have been recorded on a Finnigan LCQ Deca (ThermoQuest).

X-ray Measurements: For each data collection a single crystal was mounted on a *micro mount* and all geometric and intensity data were taken from this sample. Data collections were carried out on a Stoe IPDS2 diffractometer equipped with a 2-circle goniometer and an area detector at 100(2) K using MoK_α radiation (λ = 0.71073 Å) for **2**, and on a Stoe StadiVari diffractometer equipped with a 4-circle goniometer and a DECTRIS Pilatus 200K detector using CuK_α radiation (λ = 1.54186 Å) for **4**. The data sets were corrected for absorption (by integration), *Lorentz* and polarisation effects. The structures were solved by direct methods (SHELXT)[16] and refined using alternating cycles of least-squares refinements against F^2 (SHELXL2017/1).[17] C-bonded H atoms were included to the models in calculated positions, N-bonded H atoms have been found in the difference *Fourier* lists. All H atoms were treated with the 1.2 fold isotropic displacement parameter of their bonding partner. Experimental details for each diffraction experiment are given in Table S1. For further details on structure determination and refinement cf. Table S1 (Supporting Information).

CCDC 1921445 (for **2**), 1915905 (for **3**), and 1915906 (for **4**) contain the supplementary crystallographic data for this paper. These data can be obtained free of charge from The Cambridge Crystallographic Data Centre.

White Light Interferometry (WLI): The WLI measurements were performed with New View 5010 from Zygo and a 50x-lens is used to obtain the required resolution. The reflection on the surface causes interference, which is analyzed and calculated as a height profile. With a scan length of 5 µm in vertical direction the height of the nanoimprinted polymer blends was determined.

Scanning Electron Microscopy (SEM): For width measurements of the nanoimprinted polymer blends, SEM pictures with a magnification of 60.000 were recorded with the S-4000 from Hitachi. The width of the nanoimprinted polymer blends was determined by averaging the width by using the software ImageJ (Fiji bundle version 1.52i).

Fluorescence Microscopy (FM): A Leica fluorescence microscope was used to make the embedded compounds **2** and **4** visible. The Leica FM is operated with an UV-lamp, for which the excitation wavelength is around 360–380 nm.

Acknowledgments

The authors would like to thank the program MASH from the University of Kassel for financial support. Moreover, funding by the Deutsche Forschungsgemeinschaft (PI 353/11-1 and CRC 1319) is gratefully acknowledged. Furthermore, the authors would like to thank Prof. Maniak for permission to use the FM and Marcus Soter for his commitment in the lab.

Keywords: Phospholes · Reverse nanoimprint lithography · Fluorescence · Silicon · Solid-state structures

[1] a) T. Baumgartner, R. Réau, *Chem. Rev.* **2006**, *106*, 4681–4727; b) M. P. Duffy, W. Delaunay, P. A. Bouit, M. Hissler, *Chem. Soc. Rev.* **2016**, *45*, 5296–5310; c) M. Hissler, P. W. Dyer, R. Reau, *Top. Curr. Chem.* **2005**, *250*, 127–163.

[2] a) Y. Matano, H. Imahori, *Org. Biomol. Chem.* **2009**, *7*, 1258–1271; b) M. A. Shameem, A. Orthaber, *Chem. Eur. J.* **2016**, *22*, 10718–10735; c) E. Öberg, H. Appelqvist, K. P. R. Nilsson, *Front. Chem.* **2017**, *5*, 28.

[3] a) C. Hay, M. Hissler, C. Fischmeister, J. Rault-Berthelot, L. Toupet, L. Nyulaszi, R. Reau, *Chem. Eur. J.* **2001**, *7*, 4222–4236; b) T. Baumgartner, T. Neumann, B. Wirges, *Angew. Chem. Int. Ed.* **2004**, *43*, 6197–6201; *Angew. Chem.* **2004**, *116*, 6323–6328; c) X. He, T. Baumgartner, *RSC Adv.* **2013**, *3*, 11334–11350; d) Y. Ren, A. Orthaber, R. Pietschnig, T. Baumgartner, *Dalton Trans.* **2013**, *42*, 5314–5321.

[4] a) S. Y. Chou, P. R. Krauss, P. J. Renstrom, *Science* **1996**, *272*, 85–87; b) S. Y. Chou, US005772905A, **1998**; c) B. D. Gates, Q. Xu, M. Stewart, D. Ryan, C. G. Willson, G. M. Whitesides, *Chem. Rev.* **2005**, *105*, 1171–1196; d) K. P. Herlihy, J. Nunes, J. M. DeSimone, *Langmuir* **2008**, *24*, 8421–8426; e) Z. Xu, H.-Y. Wu, U. Ali, J. Jiang, B. Cunningham, L. Liu, *J. Nanophot.* **2011**, *5*, 053526; f) H. Hauser, N. Tucher, K. Tokai, P. Schneider, C. Wellens, A. Volk, S. Seitz, J. Benick, S. Barke, *J. Micro/Nanolith. MEMS MOEMS* **2015**, *14*, 031210.

[5] S. Reuter, M. A. Smolarczyk, A. Istock, U.-M. Ha, O. Schneider, N. Worapattrakul, S. Nazemroaya, H. Hoang, L. Gomer, F. Pilger, M. Maniak, H. Hillmer, *J. Nanopart. Res.* **2017**, *19*, 184.

[6] U. Ha, B. Kaban, A. Tomita, K. Krekić, D. Klintuch, R. Pietschnig, A. Ehresmann, D. Holzinger, H. Hillmer, *Appl. Nanosci.* **2018**, *8*, 1161–1169.

[7] I. G. M. Campbell, R. C. Cookson, M. B. Hocking, A. N. Hughes, *J. Chem. Soc.* **1965**, 2184–2193.

[8] D. Klintuch, K. Krekić, C. Bruhn, Z. Benkő, R. Pietschnig, *Eur. J. Inorg. Chem.* **2016**, *5*, 718–725.

[9] M. Schirmer, B. Schirmer in *Product information Photoresists*, Allresist, www.allresist.com, **2018**.

[10] G. Bousrez, F. Jaroschik, A. Martinez, D. Harakat, E. Nicolas, X. F. Le Goff, J. Szymoniak, *Dalton Trans.* **2013**, *42*, 10997–11004.

[11] G. Märkl, R. Potthast, *Angew. Chem. Int. Ed. Engl.* **1967**, *6*, 86.

[12] W. Kuchen, H. Buchwald, *Chem. Ber.* **1958**, *91*, 2296–2304.

[13] a) C. B. Ziegler, S. M. Harris, J. E. Baldwin, *J. Org. Chem.* **1987**, *52*, 443–446; b) J. Matsuoka, Y. Matsuda, Y. Kawada, S. Oishi, H. Ohno, *Angew. Chem. Int. Ed.* **2017**, *56*, 7444–7448; *Angew. Chem.* **2017**, *129*, 7444–7448.

[14] M. L. N. Rao, S. S. Islam, P. Dasgupta, *RSC Adv.* **2015**, *5*, 78090–78098.

[15] T. W. Odom, J. C. Love, D. B. Wolfe, K. E. Paul, G. M. Whitesides, *Langmuir* **2002**, *18*, 5314–5320.

[16] G. M. Sheldrick, *Acta Crystallogr., Sect. A: Found. Adv.* **2015**, *71*, 3–8.

[17] G. M. Sheldrick, *Acta Crystallogr., Sect. A* **2008**, *64*, 112–122.

Received: July 8, 2019